Searching for scalar field dark matter using cavity resonators and capacitors

V. V. Flambaum,[1,*] B. T. McAllister,[2,3,†] I. B. Samsonov,[1,‡] and M. E. Tobar[2,§]

[1]*School of Physics, University of New South Wales, Sydney 2052, Australia*

[2]*ARC Centre of Excellence For Engineered Quantum Systems and ARC Centre of Excellence For Dark Matter Particle Physics, QDM Laboratory, Department of Physics, University of Western Australia, 35 Stirling Highway, Crawley WA 6009, Australia*

[3]*ARC Centre of Excellence for Dark Matter Particle Physics, Centre for Astrophysics and Supercomputing, Swinburne University of Technology, John St, Hawthorn VIC 3122, Australia*

(Received 20 July 2022; accepted 8 September 2022; published 26 September 2022)

We establish new experiments to search for dark matter based on a model of a light scalar field with a dilaton-like coupling to the electromagnetic field, which is strongly motivated by superstring theory. We estimate the power of the photon signal in the process of a nonresonant scalar-photon transition and in a cavity resonator permeated by electric and magnetic fields. We show that existing cavity resonators employed in experiments like ADMX have a low but nonvanishing sensitivity to the scalar-photon coupling. As a result, by repurposing the results of the ADMX experiment, we find new limits on the scalar-photon coupling in the range of the scalar field masses from 2.7 to 4.2 μeV. We discuss possible modifications of this experiment, which enhance the sensitivity to the scalar field dark matter. We also propose a broadband experiment for scalar field dark matter searches based on a high-voltage capacitor. The estimated sensitivity of this experiment exceeds that of the experiment based on molecular spectroscopy by nearly 2 orders of magnitude.

DOI: 10.1103/PhysRevD.106.055037

I. INTRODUCTION

Scalar and pseudoscalar fields are considered as leading candidates for dark matter (DM) particles. A widely known example of a pseudoscalar particle as an extension of the Standard Model is the QCD axion, predicted in Refs. [1–7]. The axion-photon interaction $g_{a\gamma\gamma}a\vec{E}\cdot\vec{B}$ suggests that the axion field a may be converted into photons in an electric ($\vec{E}$) or magnetic ($\vec{B}$) field. A technique for detecting axions that utilizes this effect was proposed by Sikivie in Refs. [8,9]. Although the axion field has not been detected yet, the allowed values of the axion-photon coupling constant $g_{a\gamma\gamma}$ are highly constrained from a number of experiments, such as ADMX [10–18], ORGAN [19,20], CAST [21–23], and light-shining-through-a-wall experiments [24].

The scalar field counterpart of the axion is the dilaton ϕ [25], which couples to the electromagnetic field through the operator $g_{\phi\gamma\gamma}\phi(B^2-E^2)$ with the dimensionful coupling constant $g_{\phi\gamma\gamma}$. The dilaton field extension of the Standard Model is strongly motivated by superstring theory; see, e.g., Refs. [26–31]. Moreover, the scalar-photon interaction serves as a window for possible physical manifestations in chameleon models of gravity; see, e.g., Ref. [32] for a review. In contrast with the axion, the dilaton mass is much less theoretically constrained, and this represents a challenge for experimentalists to look for such particles over a wide range of values of the mass and coupling constant.

Both axion and dilaton fields are supposed to be light enough to exhibit wave-like properties. In particular, assuming that the scalar field makes up the majority of cold nonrelativistic dark matter, one concludes that such dark matter is described by a coherently oscillating background field $\phi=\phi_0\cos\omega t$, with the frequency ω equal to the mass of this field. In Refs. [33–39] it was shown that a coupling of this field to photons yields potentially observable effects of oscillations of fundamental constants that might be detected with atomic clocks. Scalar-field dark matter was searched for with the use of optical cavities [40] and gravitational-wave detectors [41–43], and the corresponding astrophysical effects were discussed in Refs. [35,44]. Scalar-photon oscillations were studied in Ref. [45]. Constraints on the scalar-field dark matter coupling were found using measurements from the DAMA experiment [46,47] and from atomic and molecular spectroscopy experiments [48–52]. Limits on the scalar-photon interaction within the chameleon model of

*v.flambaum@unsw.edu.au
†ben.mcallister@uwa.edu.au
‡igor.samsonov@unsw.edu.au
§michael.tobar@uwa.edu.au

gravity were found in Refs. [53,54]. Recently, searches for scalar dark matter using photonic, atomic, and mechanical oscillators were proposed in Refs. [55].

In this paper, we consider the possibility of the detection of scalar-field dark matter using cavity resonator haloscope techniques, analogous to the axion dark matter model [8,9]. We show that axion-detecting cavity experiments like ADMX have a low but nonvanishing sensitivity to the scalar field coupling $g_{\phi\gamma\gamma}$. This allows us to find new limits on this constant by simply repurposing the results of the ADMX experiment [15,18]. Further improvements of these limits would require some modifications of the existing cavities employed in such experiments. We propose some modifications of this experiment with various configurations of electric and magnetic fields to maximize the sensitivity.

Although cavity resonators may have a good sensitivity to the scalar-photon coupling $g_{\phi\gamma\gamma}$, they usually only allow one to explore a relatively narrow band of frequencies, while the range of allowed masses of DM particles is very wide. In this respect, broadband experiments are necessary for studying the scalar-field dark matter model. We propose one such experiment that utilizes the effect of the transformation of the scalar field into a photon in a strong electric field inside a capacitor. We show that light scalar-field dark matter should induce a detectable oscillating electric field in the capacitor. We expect that this technique should improve existing limits on $g_{\phi\gamma\gamma}$ found in Refs. [48–52] from atomic and molecular spectroscopy experiments.

The rest of the paper is organized as follows. In Sec. II we develop analytical expressions for the power of the photon signal from the scalar-photon transformation. Here we consider both a nonresonant transition in electric and magnetic fields and a transformation inside cavity resonators. We also provide numerical estimates for the power of this transformation in a cavity similar to the one used in the ADMX experiment. In Sec. III we find new constraints on the scalar-photon coupling constant by repurposing the results of the ADMX experiment and propose new experiments with enhanced sensitivity to scalar-field dark matter. Here we also present a new experimental approach for the broadband detection of scalar-field dark matter with the use of a capacitor sourced by a high-voltage DC power unit and compare the projected sensitivity with the limits from other experiments. Section IV is devoted to a summary and discussion of the results of this work.

In this paper we use natural units with $\hbar = c = \epsilon_0 = \mu_0 = 1$. The results of numerical estimates will be represented in SI units as well.

II. SCALAR-PHOTON TRANSFORMATION

A. Scalar-photon interaction

In this subsection we introduce the dilaton-like interaction of the scalar field with the electromagnetic field and derive the corresponding modifications of the Maxwell equations. We show that the scalar-field dark matter interaction with the permanent electric and magnetic fields serves as a source for electromagnetic waves.

1. Interaction with background scalar field

In vacuum, the interaction of the electromagnetic field $F_{\mu\nu}$ with a real scalar field ϕ is described by the Lagrangian

$$\mathcal{L} = -\frac{1}{4}F_{\mu\nu}F^{\mu\nu} - \frac{g_{\phi\gamma\gamma}}{4}\phi F_{\mu\nu}F^{\mu\nu}, \tag{1}$$

with a dimensionful coupling constant $g_{\phi\gamma\gamma}$. The scalar field ϕ here is considered as a background field obeying the Klein-Gordon equation $(\Box + m_\phi^2)\phi = 0$ with mass m_ϕ. In this paper, we consider a plane-wave solution for the scalar field,

$$\phi = \mathrm{Re}[\phi_0 e^{i(\vec{p}\cdot\vec{x}-\omega t)}], \tag{2}$$

with momentum $\vec{p}$ and energy $\omega = \sqrt{p^2 + m_\phi^2}$.

In general, dark matter particles may either be produced in decays of Standard Model particles or have a primordial origin. In the former case these particles are usually ultrarelativistic, while in the latter case they contribute to the cold dark matter. If these particles saturate the local dark matter density $\rho_{\mathrm{DM}} = 0.45\ \mathrm{GeV/cm^3}$, the amplitude of the scalar field (2) may be written as

$$\phi_0 = \frac{\sqrt{2\rho_{\mathrm{DM}}}}{m_\phi}. \tag{3}$$

The momentum of such particles may be written as $\vec{p} = \omega\vec{\beta}$, with $\beta = 10^{-3}c$ being the virial velocity in our Galaxy.

In this subsection, however, we consider the general case with an arbitrary DM particle velocity. The ultrarelativistic case will be discussed at the end of this section with a reference to the CAST experiment [21–23] which may detect scalar DM particles emitted from the Sun.

2. Modifications of Maxwell's equations in a medium

In a medium with dielectric constant ϵ and magnetic susceptibility μ, the Lagrangian (1) becomes

$$\mathcal{L} = \frac{1}{2}\left(\epsilon\vec{E}^2 - \frac{1}{\mu}\vec{B}^2\right) + \frac{1}{2}g_{\phi\gamma\gamma}\phi(\vec{E}^2 - \vec{B}^2), \tag{4}$$

where $\vec{E} = -\nabla\Phi - \partial_t\vec{A}$ and $\vec{B} = \nabla\times\vec{A}$ are electric and magnetic fields, respectively. The corresponding modifications of Maxwell's equations are

$$\nabla\cdot(\epsilon\vec{E} + g_{\phi\gamma\gamma}\phi\vec{E}) = 0, \tag{5a}$$

$$\nabla \times (\mu^{-1}\vec{B} + g_{\phi\gamma\gamma}\phi\vec{B}) - \partial_t(\epsilon\vec{E} + g_{\phi\gamma\gamma}\phi\vec{E}) = 0, \quad (5b)$$

$$\nabla \times \vec{E} + \partial_t\vec{B} = 0, \quad (5c)$$

$$\nabla \cdot \vec{B} = 0. \quad (5d)$$

Consider background static electric $\vec{E}_0$ and magnetic $\vec{B}_0$ fields. Equations (5a) and (5b) suggest that the scalar field ϕ interacting with these background fields serves as a source of effective electric charge and current densities:

$$\rho_\phi = -g_{\phi\gamma\gamma}\nabla \cdot (\phi\vec{E}_0), \quad (6a)$$

$$\vec{j}_\phi = g_{\phi\gamma\gamma}\vec{E}_0\partial_t\phi - g_{\phi\gamma\gamma}\nabla \times (\phi\vec{B}_0). \quad (6b)$$

With these sources, Eqs. (5a) and (5b) may be cast in the form

$$\nabla \cdot (\epsilon\vec{E}) = \rho_\phi, \quad (7a)$$

$$\nabla \times (\mu^{-1}\vec{B}) - \partial_t(\epsilon\vec{E}) = \vec{j}_\phi. \quad (7b)$$

Note that ρ_ϕ and j_ϕ satisfy the continuity equation, $\partial_t\rho_\phi + \nabla \cdot \vec{j}_\phi = 0$.

B. Nonresonant transformation power in static electric and magnetic fields

In this subsection, we find a solution of Eqs. (7a) and (7b) that will be applied to calculate of the scalar-photon transformation power. This derivation is similar to that for the axion-photon transformation presented in Ref. [56].

In what follows, we assume that ϵ and μ are constant over space and time. Then, in the Lorentz gauge, $\epsilon\mu\partial_t\Phi + \nabla \cdot \vec{A} = 0$, the Maxwell equations (7a) and (7b) imply

$$(-\nabla^2 + \epsilon\mu\partial_t^2)\Phi = \epsilon^{-1}\rho_\phi, \quad (8)$$

$$(-\nabla^2 + \epsilon\mu\partial_t^2)\vec{A} = \mu\vec{j}_\phi, \quad (9)$$

with ρ_ϕ and j_ϕ given by Eqs. (6a) and (6b).

To derive the power of radiation from the scalar-to-photon transformation it is sufficient to consider only the equation for the vector potential (9) because it is possible to show that the contribution with ρ_ϕ drops out from the Pointing vector at large distance from the source (in the wave zone); see, e.g., Ref. [57].

We will look for a solution of Eq. (9) within the ansatz $\vec{A}(x,t) = \mathrm{Re}[\vec{A}(x)e^{-i\omega t}]$, with $\vec{A}(x)$ obeying

$$(-\nabla^2 - \epsilon\mu\omega^2)\vec{A}(x) = \mu\vec{j}_\phi(x), \quad (10a)$$

$$\vec{j}_\phi(x) = -g_{\phi\gamma\gamma}\phi_0 e^{i\vec{p}\cdot\vec{x}}[i\omega\vec{E}_0 + (\nabla + i\vec{p}) \times \vec{B}_0]. \quad (10b)$$

Here the plane-wave solution for the scalar field (2) has been employed. Making use of the Fourier transform for the external magnetic field, $\vec{B}_0(x) = \int d^3x e^{i\vec{q}\cdot\vec{x}}\vec{B}_0(q)$, the last term in Eq. (10b) may be written as $(\nabla + i\vec{p}) \times \vec{B}_0(x) = i\int d^3x e^{i\vec{q}\cdot\vec{x}}(\vec{q} + \vec{p}) \times \vec{B}_0(q)$. Here $\vec{p}$ represents the scalar field momentum, while $\vec{q}$ is the momentum carried by the external magnetic field $\vec{B}_0$. We will keep both of these momenta because either of these terms may be leading. In particular, in helioscope experiments like CAST, the scalar-field momentum is supposed to be in the keV range, and the condition $p \gg q$ is satisfied. In searches for ultralight ($m_\phi \ll 10^{-6}$ eV) Galactic halo scalar dark matter, the opposite condition may be satisfied, $p \ll q$. In microwave cavities like the one in the ADMX experiment, these two terms may be comparable, $p \sim q$.

The solution of Eq. (10a) may be written in terms of Green's function,

$$\vec{A}(x) = \frac{\mu}{4\pi}\int_V d^3x' \frac{e^{ik|\vec{x}-\vec{x}'|}}{|\vec{x}-\vec{x}'|}\vec{j}_\phi(x'), \quad (11)$$

where $k = \sqrt{\epsilon\mu}\omega$. The integration is performed over the volume V with nonvanishing electric field $\vec{E}_0$ and magnetic field $\vec{B}_0$. At large distance, $r \equiv |\vec{x}| \gg V^{1/3}$, this solution is approximated as

$$\vec{A}(\vec{x}) = \mu\frac{e^{ikr}}{4\pi r}\vec{j}_\phi(k) + O\left(\frac{1}{r^2}\right), \quad (12)$$

where

$$\vec{j}_\phi(k) = \int_V d^3x e^{-i\vec{k}\cdot\vec{x}}\vec{j}_\phi(x) = -ig_{\phi\gamma\gamma}\phi_0\int_V d^3x e^{i(\vec{p}-\vec{k})\vec{x}}[(\vec{p} - i\nabla) \times \vec{B}_0 + \omega\vec{E}_0]. \quad (13)$$

Here $\vec{p} = \omega\vec{\beta}$, $\vec{x} = r\vec{n}$, and $\vec{k} = k\vec{n}$, with a unit vector $\vec{n}$.

The power of electromagnetic radiation per solid angle in the direction $\vec{n}$ is [56]

$$\frac{dP}{d\Omega} = \lim_{r\to\infty}\langle\vec{n} \cdot (\vec{E} \times \vec{H})\rangle r^2 = \frac{\mu k\omega}{32\pi^2}|\vec{n} \times \vec{j}_\phi(k)|^2, \quad (14)$$

where $\langle\ldots\rangle$ denotes the time average. The power of the scalar-photon transition is obtained upon integration of Eq. (14) over the solid angle Ω,

$$P = \frac{g_{\phi\gamma\gamma}^2\rho_{\mathrm{DM}}}{16\pi^2\epsilon}\int d^3k\delta(|\vec{k}| - \omega) \times \left|\int_V d^3x e^{i(\vec{p}-\vec{k})\cdot\vec{x}}\vec{n} \times [\vec{E}_0 + (\vec{\beta} - i\omega^{-1}\nabla) \times \vec{B}_0]\right|^2. \quad (15)$$

Here we made use of the relation (3). Using a similar relation for the energy flux of the scalar field, $\vec{\mathcal{P}} = \frac{1}{2}\phi_0^2\omega^2\vec{\beta}$, we also find the differential cross section for the scalar field to photon transformation,

$$\frac{d\sigma}{d\Omega} = \frac{1}{|\vec{\mathcal{P}}_\phi|}\frac{dP}{d\Omega} = g_{\phi\gamma\gamma}^2\frac{\mu k\omega}{16\pi^2\beta} \times\left|\int_V d^3x e^{i(\vec{p}-\vec{k})\cdot\vec{x}}\vec{n}\times[\vec{E}_0+(\vec{\beta}-i\omega^{-1}\nabla)\times\vec{B}_0]\right|^2. \quad (16)$$

The results for the differential cross section (16) and power (15) are very similar to the corresponding expressions for the axion-photon transformation found in Refs. [8,9]. However, here the roles of external electric and magnetic fields are swapped. In particular, when the electric field is vanishing (as is the case in many cavity haloscope experiments) the cross section (16) depends on the angle between the applied magnetic field $\vec{B}_0$ and the scalar field velocity, $|\vec{B}_0\times\vec{\beta}|^2 = B_0^2\beta^2\sin^2\theta$. As a result, the factor $\sin^2\theta$ should result in daily and annual modulations of the expected signal from the scalar field to photon transformation. The cross section (16) is suppressed by the factor $\beta^2 \sim 10^{-6}$ as compared with the axion-photon transformation cross section studied in Refs. [8,9].

Helioscopes, however, can detect scalar and pseudoscalar particles with equal efficiency. Indeed, the CAST experiment [21–23] aims at detecting axions produced by the Sun with energies of order 1 keV. In contrast with galactic halo dark matter, such axions are ultrarelativistic with $\beta \approx 1$. Moreover, since this helioscope is based on a moving platform and is aimed at the Sun, the applied magnetic field is always perpendicular to the axion or scalar field momentum, $\sin\theta \approx 1$. Thus, all constraints found by the CAST experiment [23] on the axion-photon coupling constant $g_{a\gamma\gamma}$ literally apply to the scalar field coupling $g_{\phi\gamma\gamma}$. The corresponding limits on $g_{\phi\gamma\gamma}$ are given in Fig. 1.

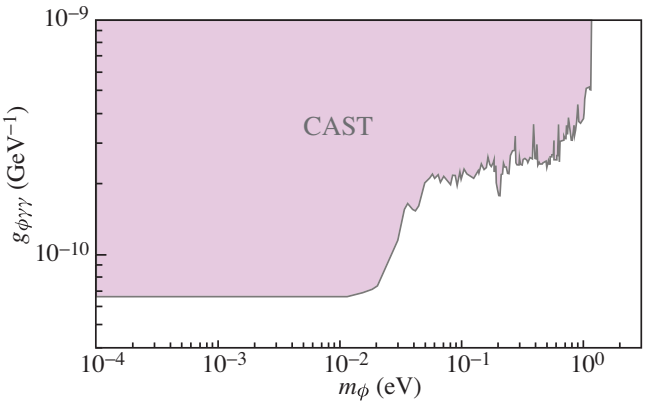

FIG. 1. Upper limits on the coupling $g_{\phi\gamma\gamma}$ derived from the results of the CAST experiment [23].

Note that in Ref. [58] it was shown that an interaction similar to that in Eqs. (6a) and (6b) and (7a) and (7b) also appears in the axion electrodynamics with magnetic monopoles. Therefore, the nondetection of solar axions in the CAST experiment is consistent with the nonobservation of magnetic monopoles.

The opposite case with vanishing external magnetic field and nonzero electric field corresponds to the scalar field to photon transformation in matter. In this case, the role of the electric field E_0 is played by the internal Coulomb fields in atoms and molecules. The possibility of detecting this effect in the DAMA experiment was discussed in Refs. [46,47]. In contrast with the axion case, however, we expect no daily or annual modulation of the signal because the power of the produced electromagnetic field is independent of $\beta\sin\theta$; see Eq. (15).

Note also that astrophysical constraints on the scalar field coupling $g_{\phi\gamma\gamma}$ were studied in a recent paper [44].

C. Transformation in a cavity resonator

In Refs. [8,9] it was shown that axion dark matter could be effectively detected with the use of cavity resonators. Such cavity resonators have been employed, e.g., in the ADMX [10–18] and ORGAN [19,20] experiments. In this subsection, we show that the cavity resonator technique appears to be efficient for measuring the scalar-photon coupling $g_{\phi\gamma\gamma}$ as well. We calculate the power of the photon signal from the scalar-photon transformation in permanent electric and magnetic fields in such cavities.

1. Estimates of the photon signal power

Consider a cavity of volume V with static electric field $\vec{E}_0$ and magnetic field $\vec{B}_0$. The vector potential in the cavity is expanded over the cavity eigenmodes $\vec{e}_\alpha$, ($\Phi = 0$ gauge is assumed[1]),

$$\vec{A}(x,t) = \sum_\alpha \vec{e}_\alpha(x)\psi_\alpha(t), \quad (17)$$

which satisfy

$$\nabla\cdot(\epsilon\vec{e}_\alpha) = 0, \quad (18a)$$

[1]In general, this gauge is inconsistent with Eq. (8), since a nonvanishing field Φ is produced by the effective charge density ρ_ϕ. For cold dark matter described by the scalar field (2) the effective charge density may however be ignored, $\rho_\phi = 0$, as compared with the effective current $\vec{j}_\phi$, and the gauge $\Phi = 0$ may be imposed. Indeed, the effective charge density appears in the following corollary of Maxwell's equations (7a)–(7b): $\nabla^2\vec{E} - \epsilon\mu\partial_t^2\vec{E} = \mu\partial_t\vec{j}_\phi + \epsilon^{-1}\nabla\rho_\phi$. For a slowly varying electric field $\vec{E}_0$ and dielectric constant ϵ, the last term here is suppressed by the factor $\beta^2 = 10^{-6}$, where $\vec{\beta} = \vec{p}/\omega$ is the virial velocity of DM particles.

$$\nabla \times (\mu^{-1}\nabla \times \vec{e}_\alpha) - \epsilon\omega_\alpha^2 \vec{e}_\alpha = 0, \tag{18b}$$

$$\vec{n} \times \vec{e}_\alpha|_S = 0, \tag{18c}$$

$$\int_V d^3x \epsilon \vec{e}_\alpha(x)\vec{e}_\beta(x) = \delta_{\alpha\beta}, \tag{18d}$$

where S is the boundary of the cavity and $\vec{n}$ is the unit vector normal to its surface, and ω_α are the eigenfrequencies. Substituting the vector potential (17) into Eq. (7b) and making use of Eqs. (18a)–(18d), we find that the amplitude $\psi_\alpha(t)$ obeys the damped driven harmonic oscillator equation

$$\left(\frac{d^2}{dt^2} + \gamma_\alpha \frac{d}{dt} + \omega_\alpha^2\right)\psi_\alpha(t) = -g_{\phi\gamma\gamma}\phi_0 \mathrm{Re}[e^{-i\omega t}F(p)], \tag{19}$$

with

$$F(p) = \int_V d^3x e^{i\vec{p}\cdot\vec{x}}\vec{e}_\alpha \cdot [i\omega\vec{E}_0 + (\nabla + i\vec{p}) \times \vec{B}_0]. \tag{20}$$

Here γ_α is the damping constant related to the cavity quality factor as $Q_\alpha = \omega_\alpha/\gamma_\alpha$. The term with the dissipation in Eq. (19) is added manually.[2]

In resonance, $\omega_\alpha = \omega \approx m_\phi$, the steady-state solution of Eq. (19) reads

$$\psi_\alpha(t) = -\frac{g_{\phi\gamma\gamma}\phi_0}{\omega\gamma_\alpha}\mathrm{Re}[ie^{-i\omega t}F(p)] \tag{21}$$

and, making use of integration by parts with the boundary condition (18c), Eq. (20) may be cast in the form

$$F(p) = \frac{1}{\psi_\alpha}\int_V d^3x e^{i\vec{p}\cdot\vec{x}}(\vec{B}_0 \cdot \vec{B}_\alpha + \vec{E}_0 \cdot \vec{E}_\alpha). \tag{22}$$

Here $\vec{E}_\alpha = -\psi'_\alpha\vec{e}_\alpha$ and $\vec{B}_\alpha = \psi_\alpha \nabla \times \vec{e}_\alpha$ are the electric and magnetic fields of the α eigenmode in the cavity, respectively. In terms of the function (20) these fields read

$$\begin{aligned}\vec{E}_\alpha &= g_{\phi\gamma\gamma}\phi_0\gamma_\alpha^{-1}\mathrm{Re}[e^{-i\omega t}F(p)]\vec{e}_\alpha,\\ \vec{B}_\alpha &= -\frac{g_{\phi\gamma\gamma}\phi_0}{\omega\gamma_\alpha}\mathrm{Re}[ie^{-i\omega t}F(p)]\nabla \times \vec{e}_\alpha.\end{aligned} \tag{23}$$

Making use of these solutions, we find the time-averaged power from the conversion of the scalar field into the α mode of the cavity,

$$\begin{aligned}P &= \frac{\gamma_\alpha}{2}\int_V d^3x\left\langle \epsilon\vec{E}_\alpha \cdot \vec{E}_\alpha + \frac{1}{\mu}\vec{B}_\alpha \cdot \vec{B}_\alpha\right\rangle\\ &= \frac{g_{\phi\gamma\gamma}^2\phi_0^2}{2\gamma_\alpha}|F(p)|^2.\end{aligned} \tag{24}$$

Remembering that $Q_\alpha = \omega/\gamma_\alpha$ is the cavity quality factor in the mode α and $\phi_0^2 = 2\rho_{\mathrm{DM}}/m_\phi^2$, we represent Eq. (24) in the conventional form

$$P = \frac{1}{m_\phi}g_{\phi\gamma\gamma}^2\rho_{\mathrm{DM}}(B_0^2 + E_0^2)VC_\alpha Q_\alpha, \tag{25}$$

where

$$C_\alpha = \frac{1}{(B_0^2 + E_0^2)V}\frac{|\int_V d^3x e^{i\vec{p}\cdot\vec{x}}(\vec{B}_0 \cdot \vec{B}_\alpha + \vec{E}_0 \cdot \vec{E}_\alpha)|^2}{\frac{1}{2}\int_V d^3x(\mu^{-1}\vec{B}_\alpha \cdot \vec{B}_\alpha + \epsilon\vec{E}_\alpha \cdot \vec{E}_\alpha)} \tag{26}$$

is the form factor which quantifies the coupling strength of cavity eigenmode α to the external electric field $\vec{E}_0$ and magnetic field $\vec{B}_0$.

2. Coupling to external magnetic field

In axion-detecting cavities like ADMX or ORGAN, strong magnetic fields are applied while the electric field is vanishing, $\vec{E}_0 = 0$. In this case, the general expressions (25) and (26) become

$$P = \frac{1}{m_\phi}g_{\phi\gamma\gamma}^2\rho_{\mathrm{DM}}B_0^2VC_\alpha Q_\alpha, \tag{27}$$

$$C_\alpha = \frac{1}{B_0^2V}\frac{|\int_V d^3x e^{i\vec{p}\cdot\vec{x}}\vec{B}_0 \cdot \vec{B}_\alpha|^2}{\int_V d^3x\mu^{-1}\vec{B}_\alpha \cdot \vec{B}_\alpha}. \tag{28}$$

Note that the factor $e^{i\vec{p}\cdot\vec{x}}$ may be omitted if the cavity is much smaller than the scalar-field de Broglie wavelength.

The radiation power (27) may be represented in physical units (watts):

$$\begin{aligned}P = 1.3\times10^8\ \mathrm{W}&\left(\frac{g_{\phi\gamma\gamma}}{\mathrm{GeV}^{-1}}\right)^2\left(\frac{3\ \mu\mathrm{eV}}{m_\phi}\right)\left(\frac{\rho_{\mathrm{DM}}}{0.45\ \mathrm{GeV/cm}^3}\right)\\ &\times\left(\frac{B_0}{7.6\ \mathrm{T}}\right)^2\left(\frac{V}{136\ \mathrm{L}}\right)\left(\frac{C_\alpha}{0.4}\right)\left(\frac{Q_\alpha}{30000}\right).\end{aligned} \tag{29}$$

This expression is very similar to the power of the axion-to-photon conversion estimated for the ADMX experiment [15]. These expressions coincide upon the substitutions $g_{\phi\gamma\gamma} \to g_{a\gamma\gamma}$ and $m_\phi \to m_a$. However, as will be shown in Sec. III B, the value of the form factor (28) is much smaller than that for the axion.

[2]It is possible to show that the same result may be found in a more systematic way by adding to Maxwell's equations (7a) and (7b) the terms with external charges and currents arising in the cavity walls. A similar derivation based on the complex Poynting theorem was reported in Ref. [59] for axion electrodynamics.

3. Coupling to external electric field

When the external magnetic field is vanishing, $\vec{B}_0 = 0$, the general expressions (25) and (26) turn into

$$P = \frac{1}{m_\phi} g^2_{\phi\gamma\gamma} \rho_{\rm DM} E_0^2 V C_\alpha Q_\alpha, \tag{30}$$

$$C_\alpha = \frac{1}{E_0^2 V} \frac{|\int_V d^3x e^{i\vec{p}\cdot\vec{x}} \vec{E}_0 \cdot \vec{E}_\alpha|^2}{\int_V d^3x \epsilon \vec{E}_\alpha \cdot \vec{E}_\alpha}. \tag{31}$$

The latter equation shows that if the homogeneous external electric field $\vec{E}_0$ is directed along the z axis of a cylindrical cavity, the dominant cavity eigenmode is TM_{010}. The corresponding form factor reads $C_\alpha = 0.69$ for a perfect cylindrical cavity (see, e.g., Ref. [56]), or $C_\alpha = 0.4$ for the cavity employed in the ADMX experiment [15]. Assuming the latter value for the form factor, we represent the power (30) in physical units:

$$P = 38\mathrm{W} \left(\frac{g_{\phi\gamma\gamma}}{\mathrm{GeV}^{-1}}\right)^2 \left(\frac{3\ \mu\mathrm{eV}}{m_\phi}\right) \left(\frac{\rho_{\rm DM}}{0.45\ \mathrm{GeV/cm}^3}\right) \times \left(\frac{E_0}{1\ \mathrm{MV/m}}\right)^2 \left(\frac{V}{136\ \mathrm{L}}\right) \left(\frac{C_\alpha}{0.4}\right) \left(\frac{Q_\alpha}{30000}\right). \tag{32}$$

Note that here we assumed reference values for the cavity volume and quality factor as in the ADMX experiment [15,18].

Comparing Eq. (32) with Eq. (29), we conclude that the cavity resonators with a magnetic field are in general much more efficient for the detection of scalar-field dark matter.

4. Signal-to-noise ratio

The approach for detecting the scalar-field dark matter with cavity resonator is very similar to the corresponding axion-detection experiments like ADMX [17]. Therefore, the signal-to-noise ratio is given by the standard expression (see, e.g., Ref. [56])

$$\mathrm{SNR} = \frac{P}{k_B T} \sqrt{\frac{t}{b}}, \tag{33}$$

where P is the expected signal power (25), T is the total noise temperature, t is the integration time, and $b \equiv f/Q$ is the cavity bandwidth.

III. EXPERIMENTAL PROPOSALS AND CONSTRAINTS

In this section we analyze the sensitivity of axion-detection experiments to the scalar-photon coupling $g_{\phi\gamma\gamma}$. As will be shown below, it is possible to find new constraints on this coupling just by repurposing the results of the ADMX experiment. Moreover, we propose new experiments dedicated to the detection of scalar-field dark matter. We divide them into two large classes corresponding to resonant cavities and broadband detection techniques.

A. Broadband detection with a capacitor

In this subsection we show that a capacitor under a strong DC electric field may serve as a broadband experiment to search for scalar-field dark matter.

Consider a capacitor with a plate separation d charged by an external source of a high voltage V_0, as in Fig. 2. The corresponding permanent electric field strength inside the capacitor is $E_0 = V_0/d$. The interaction of the scalar-field dark matter (2) with this electric field is described by Eqs. (7a) and (7b). With no external magnetic field, $\vec{B}_0 = 0$, these equations may be cast in the form

$$\begin{aligned} \nabla \cdot (\epsilon \vec{E} + \vec{P}_\phi) &= 0, \\ \nabla(\mu^{-1}\vec{B}) - \partial_t(\epsilon \vec{E} + \vec{P}_\phi) &= 0, \end{aligned} \tag{34}$$

with

$$\vec{P}_\phi = g_{\phi\gamma\gamma} \phi \vec{E}_0 \tag{35}$$

being the effective polarization vector due to the scalar field interaction with the electric field $\vec{E}_0$. The electric field $\vec{E}$ may be expanded as $\vec{E} = \vec{E}_0 + \vec{E}_\phi$, with the background field $\vec{E}_0$. As follows from Eq. (34), the field $\vec{E}_\phi$ reads

$$\vec{E}_\phi = -\epsilon^{-1} \vec{P}_\phi = -g_{\phi\gamma\gamma} \phi \epsilon^{-1} \vec{E}_0. \tag{36}$$

This field $\vec{E}_\phi$ induces an AC voltage on the plates of the capacitor,

$$V_\phi = \vec{E}_\phi \cdot \vec{d} = -g_{\phi\gamma\gamma} \epsilon^{-1} \phi V_0. \tag{37}$$

Note that this effect depends solely on the applied voltage V_0 and may be observed practically in any capacitor.

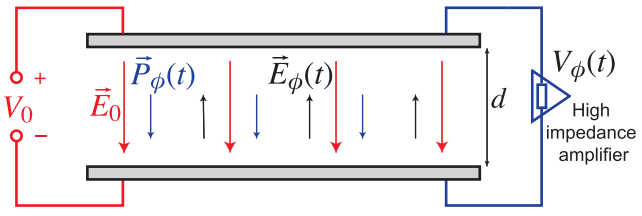

FIG. 2. Sketch of a capacitive broadband experiment for a scalar-field dark matter search. The capacitor is charged by a high-voltage V_0 producing a static electric field $\vec{E}_0$ inside the capacitor. Scalar-field dark matter interacting with $\vec{E}_0$ creates the effective polarization $\vec{P}_\phi$ and oscillating electric field $\vec{E}_\phi$. This produces an alternating voltage $V_\phi = E_\phi d$ registered through a high-impedance amplifier.

Assuming that the size of the capacitor is much smaller than the de Broglie wavelength of the scalar field, Eq. (2) may be written as $\phi = \phi_0 \cos \omega t$. In this case, Eq. (37) implies the following rms voltage due to the scalar-field dark matter:

$$\langle V_\phi \rangle = \frac{1}{\sqrt{2}} g_{\phi\gamma\gamma} \epsilon^{-1} V_0 \phi_0 = g_{\phi\gamma\gamma} \epsilon^{-1} V_0 \frac{\sqrt{\rho_{\rm DM}}}{m_\phi}, \quad (38)$$

where we made use of Eq. (3) for the scalar field amplitude ϕ_0. Equation (38) shows that the signal is linear in the scalar-photon coupling $g_{\phi\gamma\gamma}$. Thus, this experiment may have an advantage against other experiments where the signal is quadratic in $g_{\phi\gamma\gamma}$.

In our numerical estimates we assume that the applied voltage $V_0 = 600$ kV. This voltage may be produced, e.g., by a commercially available x-ray power supply [60]. For the signal detection a low-noise RF-amplifier may be used such as HFC 50D/E [61] with a spectral noise floor $\sqrt{S_V} \geq 0.2\ \text{nV}/\sqrt{\text{Hz}}$ below 50 MHz. Numerically, the spectral noise of this amplifier (in volts) may be modeled by the function

$$\sqrt{S_V} = \sqrt{\frac{7.4185 \times 10^{-14}}{f^{1.12}} + \frac{9.252 \times 10^{-19}}{f^{0.176}}}, \quad (39)$$

where f is the signal frequency measured in hertz. With the noise described by this function and the scalar field signal (38), we find the signal-to-noise ratio (SNR) for the scalar field dark matter detection experiment shown in Fig. 2:

$$\text{SNR} = g_{\phi\gamma\gamma} V_0 \sqrt{\frac{\rho_{\rm DM}}{S_V}} \left(\frac{10^6 t}{f_\phi}\right)^{\frac{1}{4}}. \quad (40)$$

Here we assume that the virialized dark matter has a bandwidth $\Delta f_\phi \sim \frac{f_\phi}{10^6}$, and the measurement time t is greater than the scalar field coherence time so that $t > \frac{10^6}{f_\phi}$. For measurement times $t < \frac{10^6}{f_\phi}$, we substitute $(\frac{10^6 t}{f_\phi})^{\frac{1}{4}} \to t^{\frac{1}{2}}$. Thus, by setting SNR $= 1$ in Eq. (40) with 30 days of integration time, we are able to find the sensitivity of this experiment; see Fig. 3.

As compared with other experiments [40,43,50–52], the detection of scalar-field dark matter with a capacitor may have advantages for various dark matter masses. In particular, the projected sensitivity is nearly 2 orders of magnitude higher than that of molecular spectroscopy experiments [51] and is comparable to that of atomic spectroscopy [52] and unequal-delay interferometer experiments [40]. Although the capacitor experiment are not as sensitive as gravitational-wave detectors [43], it would allow one to probe the region of higher scalar field mass. It should also be noted that limits from all of these experiments are significantly weaker than the constraints from the equivalence principle test [62–64].

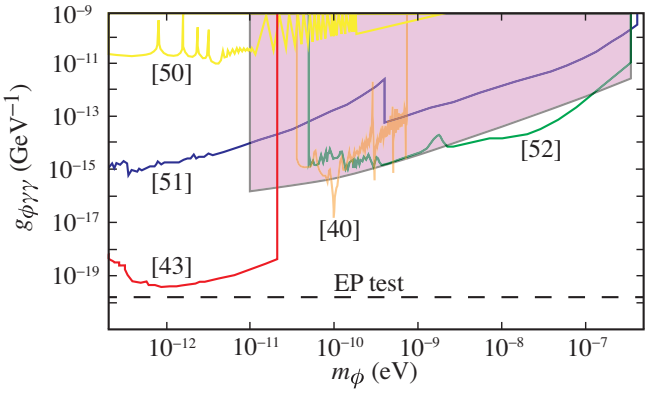

FIG. 3. Projected sensitivity of the broadband detection capacitor-based experiment (pink region) and a comparison with the constraints on the scalar-photon coupling $g_{\phi\gamma\gamma}$ from other experiments [40,43,50–52]. It is assumed that the capacitor is sourced with a 600 kV voltage and has SNR $= 1$. The dashed line represents the constraints from the equivalence principle [62–64].

Nevertheless, they provide important information about this dark matter model because they impose independent constraints on the couplings.

Note that the capacitor experiment proposed in this section may be used to probe the axion electrodynamics model [58]. In particular, all limits on $g_{\phi\gamma\gamma}$ should apply to the coupling constant $g_{a\text{AB}}$ in this model as well.

B. Limits on $g_{\phi\gamma\gamma}$ from ADMX

In typical haloscope experiments, a TM_{010} mode in a cylindrical cavity is employed, inside a solenoidal magnetic field aligned along the z axis of the cavity. If the applied magnetic field is perfectly uniform along the z direction with no fringing, then the scalar dark matter form factor (28) is exactly zero for such modes in cylindrical cavities. In fact, it does not matter how one orients the cavity with respect to the applied magnetic field, as the form factors for all modes inside a typical (haloscope-style) cylindrical cavity, with a perfectly uniform axial magnetic field, are zero.

In reality, solenoid fields are not perfectly uniform, and fringing effects exist, which create small but nonzero form factors for various modes inside resonators. For instance, for the TM_{010} mode in the ADMX Run 1c experiment, with the real ADMX solenoid, the form factor (28) is estimated as

$$C_\alpha \approx 10^{-12}, \quad (41)$$

and for the ADMX Run 1c Sidecar experiment [65]

$$C_\alpha \approx 10^{-8}. \quad (42)$$

This value imposes a strong suppression compared with the axion detection form factor $C_{\text{axion}} = 0.4$ in the ADMX experiment [15,18]. Nevertheless, it is still possible to derive new constraints on the scalar-photon coupling $g_{\phi\gamma\gamma}$ by

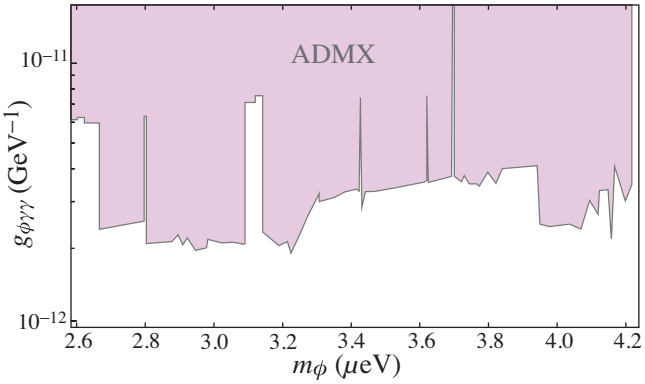

FIG. 4. Upper limits on the coupling $g_{\phi\gamma\gamma}$ as a function of mass m_ϕ. These limits are found by rescaling the corresponding constraints on the axion coupling constant $g_{a\gamma\gamma}$ (reported in Refs. [15,18]) with the constant (43).

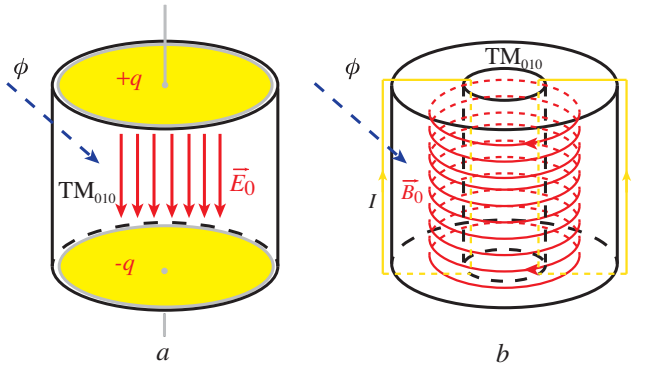

FIG. 5. Designs of cavity resonator experiments for the detection of scalar-field dark matter. (a) A cavity utilizing a strong permanent electric field $\vec{E}_0$. (b) A ring-shaped cylindrical cavity with azimuthal magnetic field $\vec{B}_0$ (red circles) created by a toroidal solenoid with current I (yellows loops).

rescaling the constraints on the axion-photon coupling reported in Refs. [15,18] by the factor

$$\kappa \equiv \sqrt{C_\alpha/0.4} = 1.6 \times 10^{-4}. \tag{43}$$

Here we assumed the value (42) for the scalar field detection form factor. The corresponding limits on $g_{\phi\gamma\gamma}$ in Fig. 4 vary from

$$g_{\phi\gamma\gamma} \lesssim 2.5 \times 10^{-12}\ \text{GeV}^{-1} \quad \text{for } m_\phi = 2.7\ \mu\text{eV} \tag{44}$$

to

$$g_{\phi\gamma\gamma} \lesssim 3.5 \times 10^{-12}\ \text{GeV}^{-1} \quad \text{for } m_\phi = 4.2\ \mu\text{eV}. \tag{45}$$

To the best of our knowledge, the coupling constant $g_{\phi\gamma\gamma}$ has not been constrained in this region yet. We hope that future experiments may further improve these constraints.

Note that in the calculation of the form factors (41) and (42) we ignored the factor $e^{i\vec{p}\cdot\vec{x}}$ in Eq. (28) because $\vec{p}\cdot\vec{x} \ll 1$. However, the terms with $\vec{p}\cdot\vec{x}$ introduce the dependence of the from factor on the scalar field momentum and may be responsible for daily and annual modulations of the signal. Moreover, such terms may produce nonvanishing form factors for some of the modes in the cavity. In particular, we find that the TE_{111} mode has a form factor $C \approx 1.7 \times 10^{-6}$ when the momentum p is aligned along the x direction of the cavity. Given this value of the form factor, the constraints in Fig. 4 could be further improved if this mode were measured in the ADMX experiment.

C. New cavity resonator proposals

Equations (41) and (42) show that the cavity resonator in the ADMX experiment has a low sensitivity to the scalar field coupling constant $g_{\phi\gamma\gamma}$. In this subsection, we discuss some proposals of cavity resonators with maximized sensitivity to scalar-field dark matter.

Equations (25) and (26) show that the role of electric and magnetic fields is swapped as compared with the corresponding expressions in the axion cavity experiment proposals [8,9]. Therefore, to maximize the sensitivity to scalar-field dark matter one may consider a cylindrical cavity resonator with an axial static electric field $\vec{E}_0$; see Fig. 5(a). In such a resonator, top and bottom caps play the role of the capacitor plates. Assuming that the strength of the applied electric field may be of order $E_0 \sim 1$ MV/m, the estimate of the signal power is given by Eq. (32). The form factor represented in Eq. (31) is maximized for the TM_{010} mode, $C_\alpha = 0.69$ for a perfect cylindrical cavity.

Cavity resonators permeated by the magnetic field are commonly used in searches for wavy dark matter because it is technically challenging to create strong electric fields in a large volume. In Fig. 5(b), we propose a magnetic-field-based cavity resonator with maximized sensitivity to the scalar-field dark matter. Such a cylindrical cavity should have the shape of a ring permeated by an azimuthal magnetic field, which could be applied with a toroidal solenoid, where current loops run through the central hole in the cavity, and around the outside. In such a cavity, TM_{010} modes are present, but unlike in the axial magnetic field they have appreciable scalar dark matter form factors, given the applied magnetic field runs in the φ direction (the same direction as the cavity mode magnetic field). Numerical simulations with the use of COMSOL software indicate that such cavities can achieve form factors close to unity, $C_\alpha \sim 1$, but the exact value of this form factor depends on the cavity parameters. This makes the cavity resonator in Fig. 5(b) very promising for future experiments searching for scalar-field dark matter with sub-meV mass.

IV. SUMMARY AND DISCUSSION

In this paper we developed a theory and a number of new experimental proposals for measuring the constant of

scalar-photon interaction $g_{\phi\gamma\gamma}$. This coupling constant quantifies the strength of the dilaton-like interaction of scalar-field dark matter with the electromagnetic field (1) that is analogous to the axion-photon coupling $g_{a\gamma\gamma}$. Similar to the axion case [8,9], scalar-field dark matter can transform into photons in strong electric and magnetic fields. We found the power of the corresponding photon signal (15) in the case of a nonresonant process and (25) in cavity resonators. In comparison with the axion case [8,9] (see also Ref. [56]), the roles of electric and magnetic fields in these expressions are swapped. As a consequence, existing cavity-based axion dark matter search experiments like ADMX or ORGAN have a low sensitivity to the scalar-photon coupling constant $g_{\phi\gamma\gamma}$. The experiments searching for Solar axions like CAST, however, possess a good sensitivity to the scalar-photon coupling $g_{\phi\gamma\gamma}$. This allowed us to find new limits on this coupling by repurposing the results of the CAST experiment; see Fig. 1.

We demonstrated that a perfect cylindrical cavity permeated by a uniform axial magnetic field does not allow one to detect scalar-field dark matter because the corresponding cavity form factor (28) vanishes identically. In actual cavities, however, the solenoid magnetic field is not perfectly uniform, and the form factor (28) acquires a small but nonvanishing value. In particular, due to the fringing of the magnetic field in the ADMX experiment [15,18] the form factor is of order $C_\alpha \approx 10^{-12}$, while in the ADMX Sidecar experiment [65] it is $C_\alpha \approx 10^{-8}$; see Eqs. (41) and (42), respectively. These values of the form factor allowed us to find new limits on the coupling $g_{\phi\gamma\gamma}$ in the scalar field mass range from 2.6 to 4.2μ eV; see Fig. 4. These limits were obtained from the corresponding constraints on the axion-photon coupling $g_{a\gamma\gamma}$ by rescaling the results of the ADMX experiment [15,18] with the coefficient (43).

To enhance the value of the form factor for scalar-field dark matter detection some modifications of the existing cavity resonators are needed. In Sec. III C we proposed a new ring-shaped cavity resonator permeated with an azimuthally oriented magnetic field induced by a toroidal solenoid. As we have shown, the from factor of such a cavity is of order $O(1)$, although its exact value depends on the particular geometry of the cavity. Alternatively, a high value of the form factor may be achieved in a cylindrical cavity permeated by a strong axial electric field, $C_\alpha = 0.69$. We hope that either of these proposals may be implemented in future experiments searching for scalar-field dark matter.

Although cavity resonators may have a good sensitivity to light scalar-field dark matter, this detection technique does not allow one to cover a wide range of masses of this particle. In Sec. III A we proposed a broadband detection technique utilizing a capacitor charged to a high voltage. The scalar field interacting with the static electric field of the capacitor induces an effective polarization and electric field in the capacitor, which oscillate with the scalar field frequency. The signal in this experiment is formed by the corresponding oscillating component of the voltage on the plates of the capacitor. Assuming reasonable values for the external voltage source and the noise level in the detector, we showed that the sensitivity to $g_{\phi\gamma\gamma}$ in this experiment may be nearly 2 orders in magnitude higher than the existing constraints on this coupling from molecular spectroscopy experiments [51] and is comparable to atomic spectroscopy experiments [52]; see Fig. 3. The advantage of this experiment is that the signal (38) has a linear dependence on the coupling constant $g_{\phi\gamma\gamma}$. This makes this technique very promising for searches for light scalar-field dark matter.

ACKNOWLEDGMENTS

We thank Yevgeny Stadnik for useful references and comments. I. B. S. is very grateful to Dmitry Budker, Gilad Perez, and Oleg Tretiak for clarifying discussions on the details of atomic and molecular spectroscopy experiments and constraints from the equivalence principle. The work of V. V. F. and I. B. S. was supported by the Australian Research Council Grants No. DP190100974 and DP200100150 and the Gutenberg Fellowship. The work of M. E. T. and B. T. M. was supported by the Australian Research Council Centre of Excellence for Engineered Quantum Systems, CE170100009 and Centre of Excellence for Dark Matter Particle Physics, CE200100008. B. T. M. is also supported by the Forrest Research Foundation. The work of I. B. S. was supported in part by the Alexander von Humboldt foundation. CAD Models for the ADMX cavity and magnetic field map were supplied by the ADMX Collaboration.

[1] R. D. Peccei and H. R. Quinn, CP Conservation in the Presence of Pseudoparticles, Phys. Rev. Lett. **38**, 1440 (1977).
[2] S. Weinberg, A New Light Boson?, Phys. Rev. Lett. **40**, 223 (1978).
[3] F. Wilczek, Problem of Strong p and t Invariance in the Presence of Instantons, Phys. Rev. Lett. **40**, 279 (1978).
[4] J. E. Kim, Weak-Interaction Singlet and Strong CP Invariance, Phys. Rev. Lett. **43**, 103 (1979).

[5] M. Shifman, A. Vainshtein, and V. Zakharov, Can confinement ensure natural *CP* invariance of strong interactions?, Nucl. Phys. **B166**, 493 (1980).
[6] A. R. Zhitnitsky, On possible suppression of the axion hadron interactions. (In Russian), Sov. J. Nucl. Phys. **31**, 260 (1980).
[7] M. Dine, W. Fischler, and M. Srednicki, A simple solution to the strong *CP* problem with a harmless axion, Phys. Lett. B **104**, 199 (1981).
[8] P. Sikivie, Experimental Tests of the "Invisible" Axion, Phys. Rev. Lett. **51**, 1415 (1983).
[9] P. Sikivie, Detection rates for "invisible"-axion searches, Phys. Rev. D **32**, 2988 (1985).
[10] C. Hagmann, P. Sikivie, N. Sullivan, D. B. Tanner, and S. Cho, Cavity design for a cosmic axion detector, Rev. Sci. Instrum. **61**, 1076 (1990).
[11] C. Hagmann, P. Sikivie, N. S. Sullivan, and D. B. Tanner, Results from a search for cosmic axions, Phys. Rev. D **42**, 1297 (1990).
[12] R. Bradley, J. Clarke, D. Kinion, L. J. Rosenberg, K. van Bibber, S. Matsuki, M. Mück, and P. Sikivie, Microwave cavity searches for dark-matter axions, Rev. Mod. Phys. **75**, 777 (2003).
[13] S. J. Asztalos *et al.*, Squid-Based Microwave Cavity Search for Dark-Matter Axions, Phys. Rev. Lett. **104**, 041301 (2010).
[14] J. Hoskins *et al.*, Search for nonvirialized axionic dark matter, Phys. Rev. D **84**, 121302 (2011).
[15] T. Braine *et al.* (ADMX Collaboration), Extended Search for the Invisible Axion with the Axion Dark Matter Experiment, Phys. Rev. Lett. **124**, 101303 (2020).
[16] C. Bartram *et al.* (ADMX Collaboration), Axion dark matter experiment: Run 1b analysis details, Phys. Rev. D **103**, 032002 (2021).
[17] R. Khatiwada *et al.* (ADMX Collaboration), Axion dark matter experiment: Detailed design and operations, Rev. Sci. Instrum. **92**, 124502 (2021).
[18] C. Bartram *et al.* (ADMX Collaboration), Search for Invisible Axion Dark Matter in the 3.3–4.2 μeV Mass Range, Phys. Rev. Lett. **127**, 261803 (2021).
[19] B. T. McAllister, G. Flower, E. N. Ivanov, M. Goryachev, J. Bourhill, and M. E. Tobar, The ORGAN experiment: An axion haloscope above 15 GHz, Phys. Dark Universe **18**, 67 (2017).
[20] A. Quiskamp, B. T. McAllister, P. Altin, E. N. Ivanov, M. Goryachev, and M. E. Tobar, Direct search for dark matter axions excluding ALP cogenesis in the 63- to 67-μeV range with the ORGAN experiment, Sci. Adv. **8**, eabq3765 (2022).
[21] K. Zioutas *et al.* (CAST Collaboration), First results from the CERN Axion Solar Telescope (CAST), Phys. Rev. Lett. **94**, 121301 (2005).
[22] S. Andriamonje *et al.* (CAST Collaboration), An improved limit on the axion-photon coupling from the CAST experiment, J. Cosmol. Astropart. Phys. 04 (2007) 010.
[23] V. Anastassopoulos *et al.* (CAST Collaboration), New CAST limit on the axion-photon interaction, Nat. Phys. **13**, 584 (2017).
[24] K. Ehret *et al.* (ALPS Collaboration), Resonant laser power build-up in ALPS: A 'Light-shining-through-walls' experiment, Nucl. Instrum. Methods Phys. Res., Sect. A **612**, 83 (2009).
[25] K. Allison, C. T. Hill, and G. G. Ross, An ultra-weak sector, the strong *CP* problem and the pseudo-Goldstone dilaton, Nucl. Phys. **B891**, 613 (2015).
[26] T. Taylor and G. Veneziano, Dilaton couplings at large distances, Phys. Lett. B **213**, 450 (1988).
[27] T. Damour and A. Polyakov, The string dilation and a least coupling principle, Nucl. Phys. **B423**, 532 (1994).
[28] T. Damour and A. M. Polyakov, String theory and gravity, Gen. Relativ. Gravit. **26**, 1171 (1994).
[29] T. Damour, F. Piazza, and G. Veneziano, Runaway Dilaton and Equivalence Principle Violations, Phys. Rev. Lett. **89**, 081601 (2002).
[30] T. Damour, F. Piazza, and G. Veneziano, Violations of the equivalence principle in a dilaton-runaway scenario, Phys. Rev. D **66**, 046007 (2002).
[31] D. B. Kaplan and M. B. Wise, Couplings of a light dilaton and violations of the equivalence principle, J. High Energy Phys. 08 (2000) 037.
[32] C. Burrage and J. Sakstein, Tests of chameleon gravity, Living Rev. Relativity **21**, 1 (2018).
[33] A. Arvanitaki, J. Huang, and K. Van Tilburg, Searching for dilaton dark matter with atomic clocks, Phys. Rev. D **91**, 015015 (2015).
[34] K. Van Tilburg, N. Leefer, L. Bougas, and D. Budker, Search for Ultralight Scalar Dark Matter with Atomic Spectroscopy, Phys. Rev. Lett. **115**, 011802 (2015).
[35] Y. V. Stadnik and V. V. Flambaum, Can Dark Matter Induce Cosmological Evolution of the Fundamental Constants of Nature?, Phys. Rev. Lett. **115**, 201301 (2015).
[36] Y. V. Stadnik and V. V. Flambaum, Improved limits on interactions of low-mass spin-0 dark matter from atomic clock spectroscopy, Phys. Rev. A **94**, 022111 (2016).
[37] Y. V. Stadnik and V. V. Flambaum, Enhanced effects of variation of the fundamental constants in laser interferometers and application to dark-matter detection, Phys. Rev. A **93**, 063630 (2016).
[38] A. Hees, J. Guéna, M. Abgrall, S. Bize, and P. Wolf, Searching for an Oscillating Massive Scalar Field as a Dark Matter Candidate Using Atomic Hyperfine Frequency Comparisons, Phys. Rev. Lett. **117**, 061301 (2016).
[39] C. J. Kennedy, E. Oelker, J. M. Robinson, T. Bothwell, D. Kedar, W. R. Milner, G. Edward Marti, A. Derevianko, and J. Ye, Precision Metrology Meets Cosmology: Improved Constraints on Ultralight Dark Matter from Atom-Cavity Frequency Comparisons, Phys. Rev. Lett. **125**, 201302 (2020).
[40] E. Savalle, A. Hees, F. Frank, E. Cantin, P.-E. Pottie, B. M. Roberts, L. Cros, B. T. McAllister, and P. Wolf, Searching for Dark Matter with an Optical Cavity and an Unequal-Delay Interferometer, Phys. Rev. Lett. **126**, 051301 (2021).
[41] A. Branca *et al.*, Search for an Ultralight Scalar Dark Matter Candidate with the Auriga Detector, Phys. Rev. Lett. **118**, 021302 (2017).
[42] H. Grote and Y. V. Stadnik, Novel signatures of dark matter in laser-interferometric gravitational-wave detectors, Phys. Rev. Res. **1**, 033187 (2019).
[43] S. M. Vermeulen *et al.*, Direct limits for scalar field dark matter from a gravitational-wave detector, Nature (London) **600**, 424 (2021).

[44] A. Caputo, G. Raffelt, and E. Vitagliano, Muonic boson limits: Supernova redux, Phys. Rev. D **105**, 035022 (2022).
[45] E. Gabrielli, K. Huitu, and S. Roy, Photon propagation in magnetic and electric fields with scalar/pseudoscalar couplings: A new look, Phys. Rev. D **74**, 073002 (2006).
[46] R. Bernabei *et al.*, Investigating pseudoscalar and scalar dark matter, Int. J. Mod. Phys. A **21**, 1445 (2006).
[47] H. B. Tran Tan, A. Derevianko, V. A. Dzuba, and V. V. Flambaum, Atomic Ionization by Scalar Dark Matter and Solar Scalars, Phys. Rev. Lett. **127**, 081301 (2021).
[48] D. Antypas, O. Tretiak, A. Garcon, R. Ozeri, G. Perez, and D. Budker, Scalar Dark Matter in the Radio-Frequency Band: Atomic-Spectroscopy Search Results, Phys. Rev. Lett. **123**, 141102 (2019).
[49] D. Antypas, O. Tretiak, K. Zhang, A. Garcon, G. Perez, M. G. Kozlov, S. Schiller, and D. Budker, Probing fast oscillating scalar dark matter with atoms and molecules, Quantum Sci. Technol. **6**, 034001 (2021).
[50] S. Aharony, N. Akerman, R. Ozeri, G. Perez, I. Savoray, and R. Shaniv, Constraining rapidly oscillating scalar dark matter using dynamic decoupling, Phys. Rev. D **103**, 075017 (2021).
[51] R. Oswald *et al.*, Search for Dark-Matter-Induced Oscillations of Fundamental Constants Using Molecular Spectroscopy, Phys. Rev. Lett. **129**, 031302 (2022).
[52] O. Tretiak, X. Zhang, N. L. Figueroa, D. Antypas, A. Brogna, A. Banerjee, G. Perez, and D. Budker, Improved Bounds on Ultralight Scalar Dark Matter in the Radio-Frequency Range, Phys. Rev. Lett. **129**, 031301 (2022).
[53] G. Rybka *et al.*, Search for Chameleon Scalar Fields with the Axion Dark Matter Experiment, Phys. Rev. Lett. **105**, 051801 (2010).
[54] I. Antoniou, Constraints on scalar coupling to electromagnetism, Gravitation Cosmol. **23**, 171 (2017).
[55] W. M. Campbell, B. T. McAllister, M. Goryachev, E. N. Ivanov, and M. E. Tobar, Searching for Scalar Dark Matter via Coupling to Fundamental Constants with Photonic, Atomic, and Mechanical Oscillators, Phys. Rev. Lett. **126**, 071301 (2021).
[56] P. Sikivie, Invisible axion search methods, Rev. Mod. Phys. **93**, 015004 (2021).
[57] L. D. Landau and E. M. Lifschits, *The Classical Theory of Fields*, Course of Theoretical Physics (Pergamon Press, Oxford, 1975), Vol. 2.
[58] A. V. Sokolov and A. Ringwald, Electromagnetic couplings of axions, arXiv:2205.02605.
[59] M. E. Tobar, B. T. McAllister, and M. Goryachev, Poynting vector controversy in axion modified electrodynamics, Phys. Rev. D **105**, 045009 (2022).
[60] Wisman high voltage power supply, https://www.wismanhv.com/Upfiles/uploadfile/202205/20220505171004558.pdf.
[61] HFC 50 D/E, dual cryogenic ultra low noise RF-amplifier, https://www.stahl-electronics.com/bilder/Datasheet_HFC50DE_2-38.pdf.
[62] G. L. Smith, C. D. Hoyle, J. H. Gundlach, E. G. Adelberger, B. R. Heckel, and H. E. Swanson, Short-range tests of the equivalence principle, Phys. Rev. D **61**, 022001 (1999).
[63] A. Hees, O. Minazzoli, E. Savalle, Y. V. Stadnik, and P. Wolf, Violation of the equivalence principle from light scalar dark matter, Phys. Rev. D **98**, 064051 (2018).
[64] S. Schlamminger, K.-Y. Choi, T. A. Wagner, J. H. Gundlach, and E. G. Adelberger, Test of the Equivalence Principle Using a Rotating Torsion Balance, Phys. Rev. Lett. **100**, 041101 (2008).
[65] C. Bartram *et al.*, Dark matter axion search using a Josephson traveling wave parametric amplifier, arXiv:2110.10262.